

See discussions, stats, and author profiles for this publication at: <https://www.researchgate.net/publication/301902152>

# Proportional-derivative linear quadratic regulator controller design for improved longitudinal motion control of unmanned aerial vehicles

Article in *International Journal of Micro Air Vehicles* · March 2016

DOI: 10.1177/1756829316638210

CITATIONS

16

READS

3,878

3 authors, including:



Kai Yit Kok

Universiti Sains Malaysia

19 PUBLICATIONS 110 CITATIONS

[SEE PROFILE](#)



Parvathy Rajendran

Universiti Sains Malaysia

153 PUBLICATIONS 982 CITATIONS

[SEE PROFILE](#)

# Proportional-derivative linear quadratic regulator controller design for improved longitudinal motion control of unmanned aerial vehicles

Kok Kai Yit, Parvathy Rajendran and Lim Kah Wee

## Abstract

This study investigates the longitudinal motion control of unmanned aerial vehicles through a simulation in MATLAB. The linear model of an unmanned aerial vehicle is applied to controllers to explicate the longitudinal motion of the unmanned aerial vehicle. The ideal performance for an unmanned aerial vehicle is to achieve the desired response instantly with 100% precision. However, currently available controllers need further improvements. Thus, a proportional-derivative linear quadratic regulator controller is developed and compared with a proportional-integral-derivative controller, a linear quadratic regulator controller, and a proportional linear quadratic regulator controller. The proportional-derivative linear quadratic regulator controller enhances the response of the system by reducing settling time by more than 95% compared with other available controllers. Additionally, the proportional-derivative linear quadratic regulator improves the root mean square error by almost 50% compared with the proportional linear quadratic regulator controller and improves rise time by almost 96% with reasonable overshoot.

## Keywords

proportional-integral-derivative, linear quadratic regulator, rise time, settling time, overshoot, micro air vehicle, unmanned aerial vehicle, longitudinal motion control

Date received: 14 April 2015; accepted: 18 February 2016

## Introduction

Small unmanned aerial vehicles (UAVs) have been widely developed in recent years and have been implemented in both military and civilian applications such as applications for search and rescue, surveillance<sup>1</sup> and reconnaissance, traffic monitoring, wild life suppression, data collection, transmission, and so on.<sup>2–4</sup> Researchers have great interest in UAV development due to the minimization of the risk factors for pilots and the drastic reduction of cost operations.<sup>5,6</sup> However, the communication link between UAVs and ground stations possesses a weighty time delay, and the unmanned characteristic of the UAV prevents its pilot from detecting its real-time motion.<sup>6</sup>

Hence, a flight control system that has excellent performance is crucial. Ultimately, a fully-autonomous system for the UAV is developed to take complete advantage of UAVs. In the meantime, computational algorithms, such as proportional-integral-derivative (PID), linear quadratic regulator (LQR), fuzzy logic, and neural network, have been studied to stabilize

UAVs during flight operation.<sup>7</sup> Currently available controllers remain to provide less than ideal performance and even small improvements on these controllers can produce a significant effect. For example, a typical military micro-air vehicle (MAV)<sup>8</sup> with a cruise speed of 87.4 m/s can decrease the distance for stabilization by 17.4 m when settling time is reduced by only 0.2 s.

The LQR controller is a well-known controller for minimizing cost functions. In vertical flight motion, the LQR controller has been tested and proven to be effective.<sup>9</sup> This controller has also been applied in various aircraft models to verify the performance of the controllers therein. Studies have been conducted on the combination of the LQR controller with a Kalman

School of Aerospace Engineering, Universiti Sains Malaysia, Engineering Campus, Pulau Pinang, Malaysia

### Corresponding author:

Parvathy Rajendran, School of Aerospace Engineering, Universiti Sains Malaysia, Engineering Campus, 14300 Nibong Tebal, Pulau Pinang, Malaysia.

Email: aeaprvathy@usm.my



filter to form a linear quadratic Gaussian (LQG) controller. The purpose of this combination is to lessen the effect of noise disturbance on the controller performance. However, the LQG controller has failed in real-time testing due to insufficient robustness.<sup>10</sup> Moreover, the response speed and stability margins of the LQG controller are lower than that of the LQR controller.<sup>11</sup>

PID controller is another commonly used controller, implemented successfully in actual aircraft control systems.<sup>12</sup> This controller is often implemented to enhance the response times of systems with first- or second-order characteristics.<sup>13</sup> The PID controller is popular because its simple structure can be easily applied with sufficient performance.

However, in analyzing the longitudinal motion of UAVs, the performance of the proportional linear quadratic regulator (P-LQR) controller is better than that of both PID and LQR controllers.<sup>14</sup> The main drawback of the P-LQR controller is with regard to overshoot. Therefore, a new controller, named the proportional-derivative linear quadratic regulator (PD-LQR) controller, for analyzing the longitudinal motion of UAVs is herein designed by combining the LQR and PD controllers. A simulation programmed using Simulink language is conducted on the proposed controller and the other controllers to identify differences in their performance. Results from the analysis show that the PD-LQR controller performs better than the other controllers.

The mathematical model of an UAV is discussed in the next section, followed by the performance indexes to be used in analysis. Then, the PID, LQR, and P-LQR controllers are described. The concept of the PD-LQR controller and the purpose for the proposed combination are explained in PD\_LQR Controller. Finally, the simulation results and analysis are discussed in detail.

## Mathematical model of UAV

A UAV is assumed to fly in a steady, level state with a constant velocity. For the present investigation on longitudinal motion, the small UAV model, Bluebird, is used. Moreover, the short-period model is herein used, as this model is more accurate for studying aircraft longitudinal motion than the phugoid model. A short period model for the Bluebird is expressed by  $L_{win}$ ,<sup>15</sup> as shown in equation (1)

$$\begin{bmatrix} \Delta \dot{a} \\ \Delta \dot{q} \end{bmatrix} = \begin{bmatrix} -5.3293 & 1 \\ -22.2728 & -4.5916 \end{bmatrix} \begin{bmatrix} \Delta a \\ \Delta q \end{bmatrix} + \begin{bmatrix} -0.5269 \\ -32.9831 \end{bmatrix} [\Delta \delta_e] \quad (1)$$

The longitudinal transfer function of this model, by using steering inertia model transfer function,<sup>7</sup> can be estimated using equation (2)

$$G(s) = \frac{329.8s + 1640.4}{s^3 + 19.92s^2 + 145.94s + 467.4} \quad (2)$$

The state matrix can then be acquired by converting the transfer function (equation 3)

$$A = \begin{bmatrix} -19.9209 & -9.1220 & -1.8259 \\ 16 & 0 & 0 \\ 0 & 16 & 0 \end{bmatrix}, B = \begin{bmatrix} 4 \\ 0 \\ 0 \end{bmatrix}, \\ C = [0 \quad 5.1550 \quad 1.6080], D = 0 \quad (3)$$

The longitudinal motion of the UAV can then be investigated using either the transfer function or the state space variables depending on controller requirements.

## Performance indexes

Generally, certain parameters defined throughout this investigation, including overshoot and control precision, have acceptable limit ranges. Any flight will not be comfortable if overshoot is severe and control precision is not low enough. Thus, the recommended acceptable range of overshoot has been set to not exceed 10%,<sup>11</sup> and control precision to not exceed  $\pm 1\%$ .<sup>16</sup> Moreover, the performance indexes for the analysis take into consideration the wide range of UAV sizes. The size of an UAV can be as small as 15 cm, as with the UAV known as MAV. Nevertheless, a MAV can fly at an average of 50 km/h.<sup>17</sup> Therefore, the expected level of precision in this study is set to  $\pm 0.001$  s.

## PID controller

Currently, the PID controller is widely used in industrial applications<sup>7</sup> due to its simplicity. This controller involves three gain parameters including proportional, integral, and derivative gains.<sup>18</sup> To minimize cost function, this controller adjusts input value to reduce the contrast between the desired value and the measured value. The equation of the PID controller can be expressed as follows<sup>19–21</sup>

$$u(t) = K_p e(t) + K \int_0^t e(\tau) d\tau + K_d \frac{de(t)}{dt} \quad (4)$$

## LQR controller

An LQR controller is a closed-loop system with an optimal control technique. The output of the system is compared to the set-point value, and feedback is returned to the system through controller gain  $K$ .<sup>18</sup> This system can be expressed in state variable form (equation 5)<sup>22,23</sup>

$$\dot{x} = Ax + Bu \quad (5)$$

Obtaining controller  $K$  is needed to achieve the desired output<sup>18</sup>; the optimal control vector (equation 6) for the state space form in a system is<sup>7,9,18,19,22–24</sup>

$$u = -Kx \quad (6)$$

The cost function known (equation 7) as the quadratic performance index needs to be reduced to acquire an optimal control signal<sup>7,9,19,22,24</sup>

$$J = \frac{1}{2} \int_0^{\infty} (x^T Q x + u^T R u) dt \quad (7)$$

$Q$  is a positive semi-definite matrix and  $R$  is a positive definite matrix. If  $Q$  is large, the state of the system  $x(t)$  must be lowered to keep  $J$  small. If  $R$  is high, the control input  $u(t)$  must be lessened to keep  $J$  small. In order to calculate optimal gain  $K$ , the algebraic Riccati equation (equation 8)<sup>22,24</sup> must be solved.

$$A^T P + PA + Q - PBR^{-1}B^T P = 0 \quad (8)$$

$K$  (equation 9) can be obtained through<sup>23</sup>

$$K = R^{-1}B^T P \quad (9)$$

Moreover, MATLAB can be used to obtain  $K$  by using command LQR ( $A$ ,  $B$ ,  $C$ ,  $D$ ,  $Q$ , and  $R$ )<sup>25,26</sup> as shown in equation (10)

$$K = [4.3957 \quad 5.3881 \quad 1.1516] \quad (10)$$

## P-LQR controller

A P-LQR controller is the combination of a proportional controller and an LQR controller. The proportional controller improves the LQR controller by shortening rise time and settling time and improving the root mean square error (RMSE). However, the proportional controller tends to increase overshoot. In this study, the proportional gain after tuning is 0.142. The flow of a P-LQR controller is shown in Figure 3.

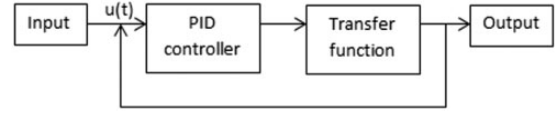


Figure 1. The flow of a PID controller.

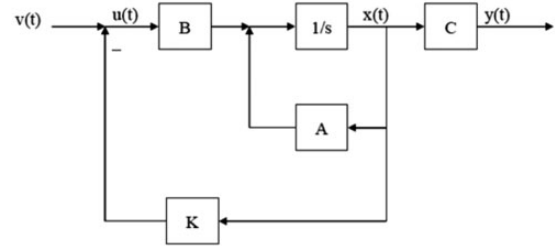


Figure 2. The flow of a LQR controller.

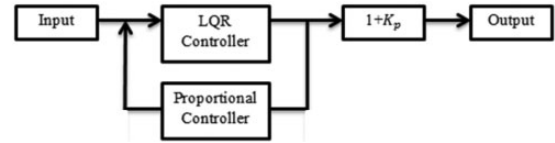


Figure 3. The flow of a P-LQR controller.

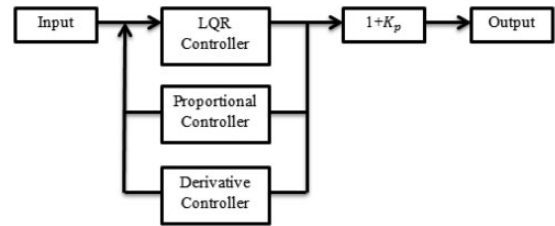


Figure 4. The flow of the PD-LQR controller.

## PD-LQR controller

To further improve the response performance in current available controllers, a combination of the LQR controller and the PD controller is proposed. The optimal gain for the LQR is obtained by solving the algebraic Riccati equation<sup>22,24</sup>; combining this with a PD controller can improve the current LQR controller response performance without affecting the desired output. A proportional controller can increase response speed and thus shorten the time needed to reach the desired output. Moreover still, another gain parameter is required to balance the desired output. The downside of this controller is its tendency to increase overshoot and make the system more unstable than before.

Hence, the derivative controller element in the proposed PD-LQR controller reduces the overshoot and makes the response smooth and stable. An integral controller is not included in this combination as it will affect the system output when it is added to an LQR controller. Figure 4 shows the flow of the PD-LQR controller.

For defining the proportional and derivative gains of the model, the Ziegler and Nichols method<sup>7,27,28</sup> is no longer suitable because the model is in a state space form. In the first place, the input from the system to the PD controller is already in a stable form. They act like a “booster” to the LQR controller, resulting in a fast and improved response performance while maintaining overshoot within the acceptable range. Tuning both proportional and derivative gains (i.e. increasing proportional gain to optimize derivative gain) indicate

that the response performance is improving, until a certain maximum value is reached and performance becomes unstable.

### Increment of proportional gain in PD-LQR

Figure 5 shows the rise time and settling time along proportional gain without the derivative controller gain. When the proportional controller increases response speed, rise time will decrease when proportional gain increases. Nonetheless, rise time will decrease to the minimum level and remain almost constant when proportional gain is further enlarged. However, this will drastically increase the overshoot of the system, as shown in Figure 6, which is characteristic of the proportional controller. The overshoot

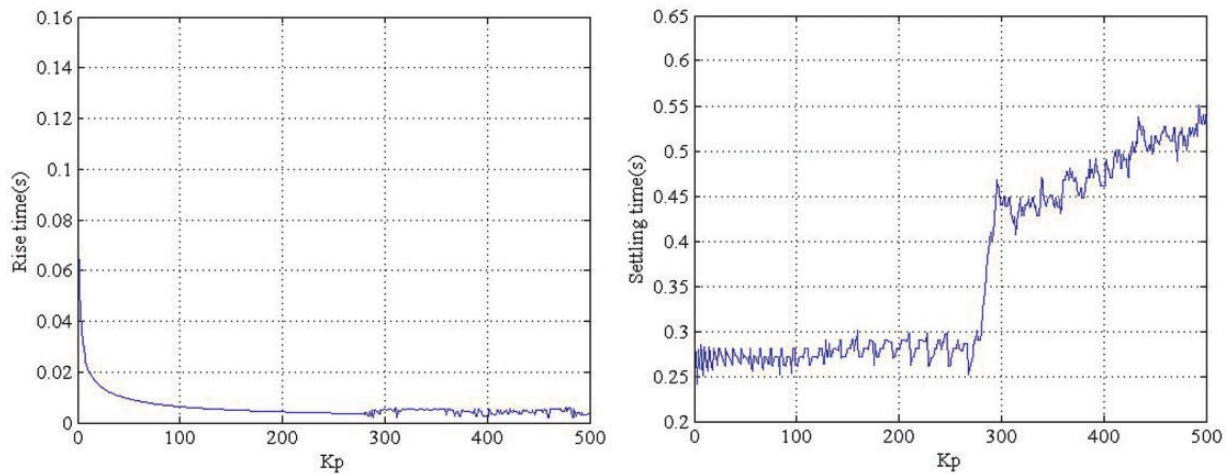


Figure 5. Rise time and settling time along proportional gain.

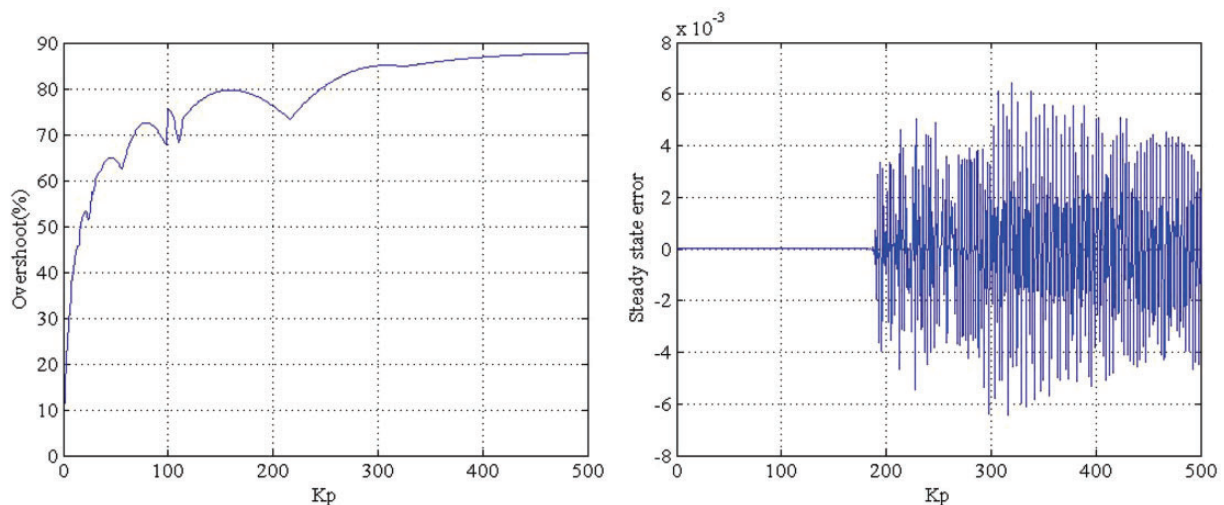
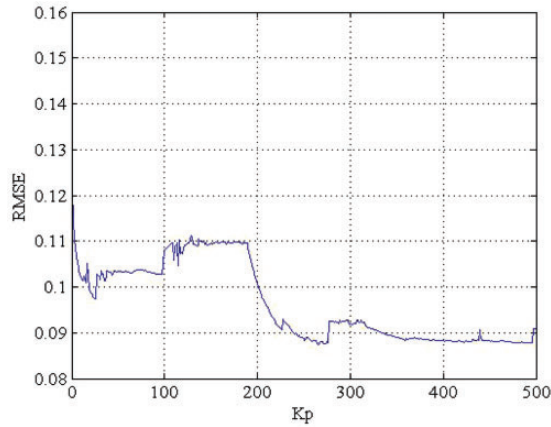


Figure 6. Overshoot and steady-state error along proportional gain.





**Figure 7.** RMSE along proportional gain.

increases sharply at the beginning but eventually converges to the maximum level.

The oscillation issue of the response becomes severe when proportional gain is high, increasing the settling time of the system even though rise time is at the minimum level. A high magnitude of overshoot when proportional gain is high also leads to a high settling time, which is pronounced when proportional gain is more than 275. The steady-state error is almost constant when proportional gain is low. Nonetheless, the system becomes unstable because of the oscillation and overshoot problems at high proportional gain. Thus, the steady-state error fluctuates (Figure 6). Additionally, RMSE exhibits only a slight improvement with the increase of proportional gain (Figure 7).

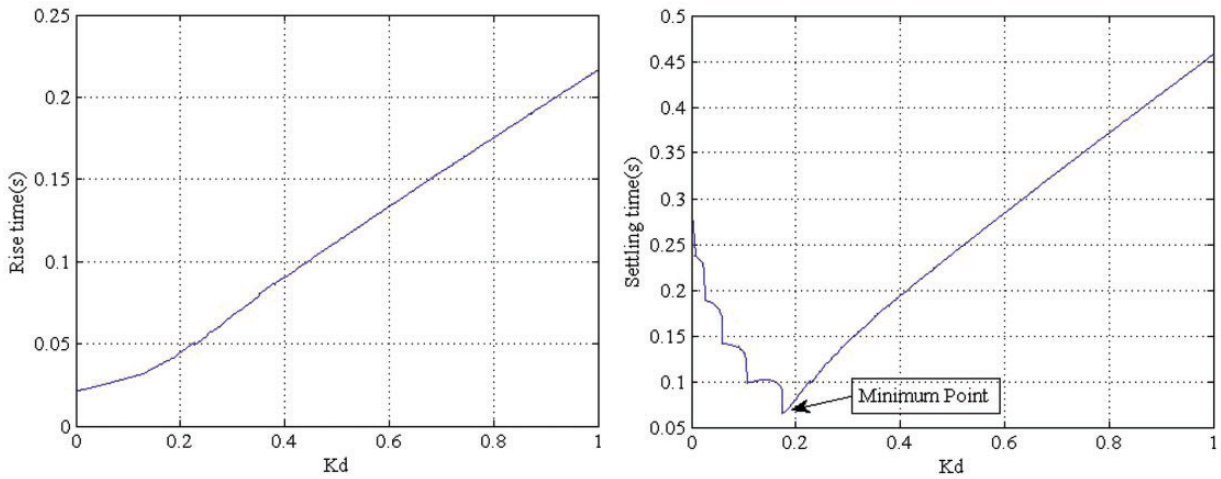


**Figure 8.** Rise time and settling time along derivative gain when proportional gain = 10.

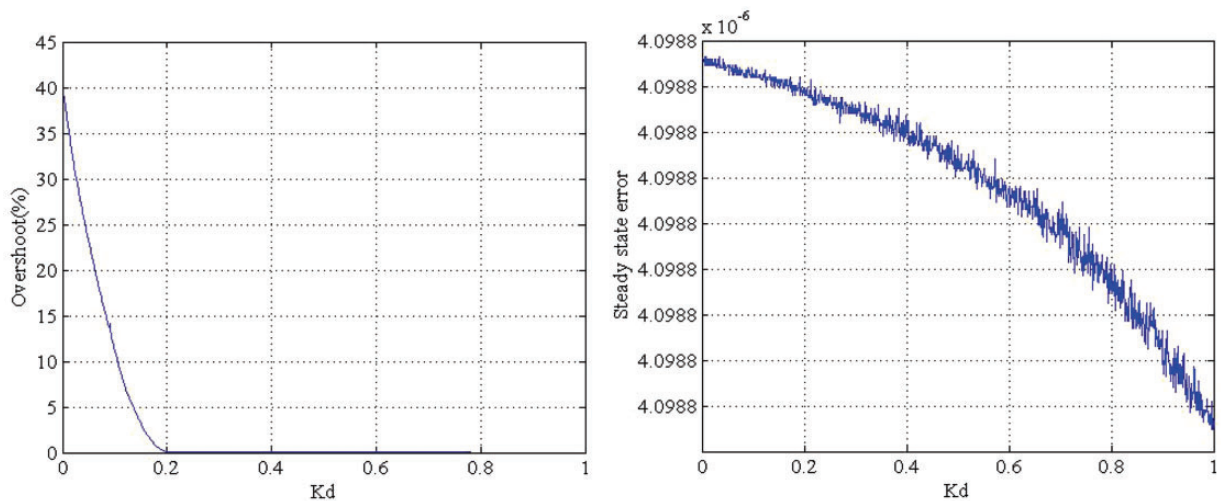


**Figure 9.** Overshoot and steady-state error along derivative gain when proportional gain = 10.

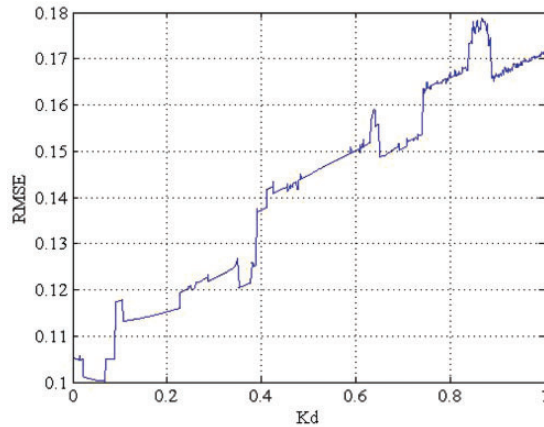


**Figure 10.** RMSE along derivative gain when proportional gain = 10.

### *Increment of derivative gain for particular proportional gain in PD-LQR*

Any proportional gain value can be optimized by adding an optimized derivative gain. The derivative controller will reduce overshoot and diminish oscillation issues caused by the proportional controller with an increase in rise time and settling time. Figures 8–10 show the response performance of the system with a proportional gain of 10 along the derivative gain.

Generally, rise time increases almost linearly from derivative gain 0 to 1 because the derivative controller tends to lessen overshoot by enlarging error correction and to make for a smooth and stable response. As a result, a longer response time is needed to achieve the desired output. The settling time is magnified with the

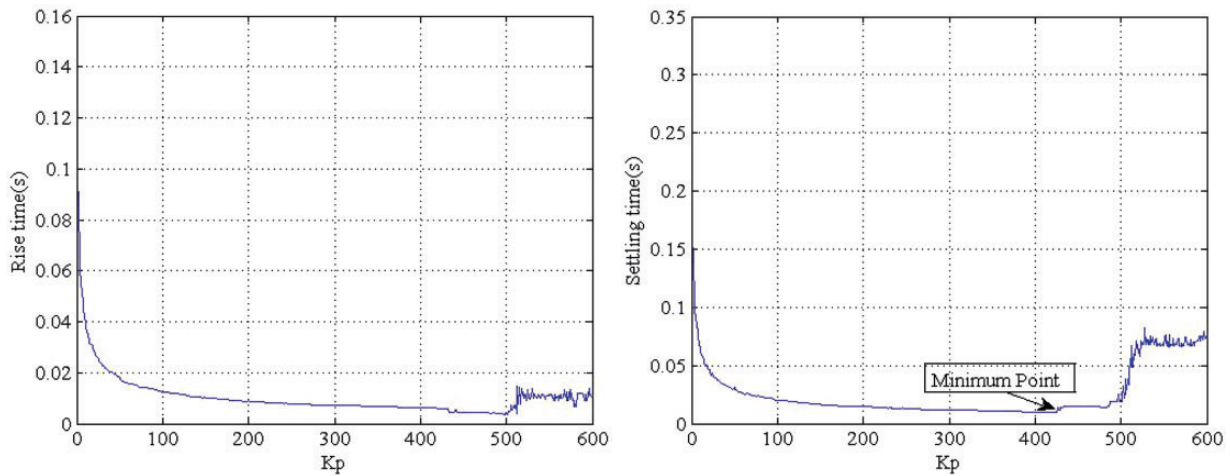


**Figure 11.** Rise time and settling time along proportional gain with optimized derivative gain.

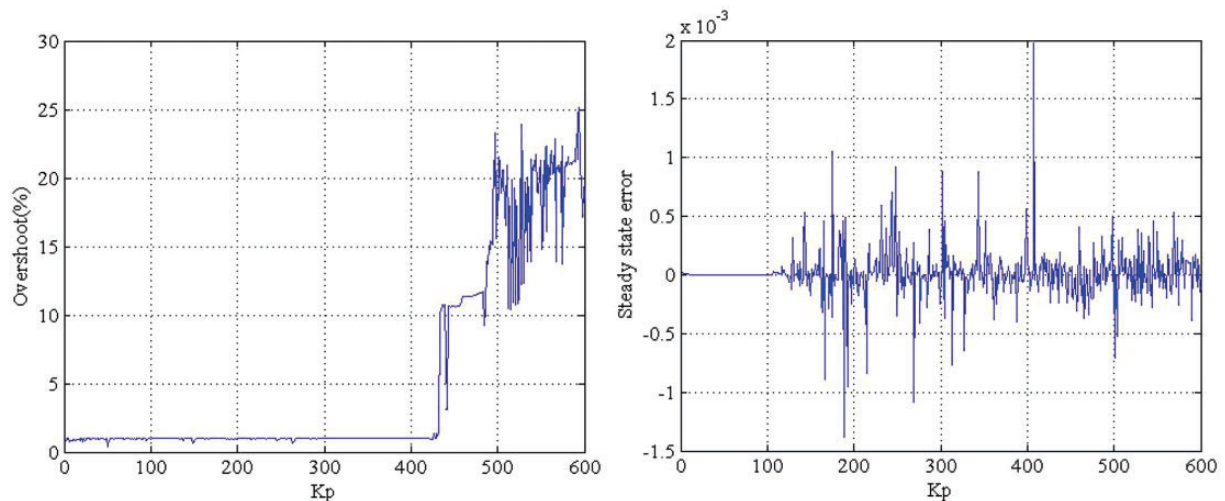


**Figure 12.** Overshoot and steady state error along proportional gain with optimized derivative gain.

rise time. However, oscillations occur in the response especially when proportional gain is high, which increases the settling time of the response. As the derivative gain increases, it eventually reduces the oscillations, reducing settling time significantly. As shown in Figure 8, settling time decreases to a minimum point before it increases. This minimum point occurs just when all oscillations are diminished and where the output would be stable afterwards and at which settling time increases in approximately the same rate as rise time.

As shown in Figure 9, the overshoot drops remarkably when derivative gain rises and remains near zero after the gain reaches a certain value. The steady-state error of the system remains near zero throughout the plot (Figure 9). Nonetheless, it is likely to decrease as the gain is enlarged. In addition, the RMSE is amplified because the slope of the response decreases as the derivative gain increases. Clearly thus, the optimum derivative gain for the given proportional gain is at the point when settling time is at the lowest limit. This point is also where the rise time and RMSE are considerably low and overshoot is significantly reduced.

#### *Increment of proportional gain with optimized derivative gain in PD-LQR*

Figures 11–13 show the response performance of the system when optimized derivative gains are applied to each of the corresponding proportional gains. Overall, a slight increase in rise time occurs after optimized derivative gain is applied in the system. Meanwhile, settling time is improved drastically especially at high proportional gain. The plot is decreasing smoothly, as in the rise time plot, which is significantly contrary to the plot in Figure 5. Nonetheless, settling time would decline to the minimum level and would climb again

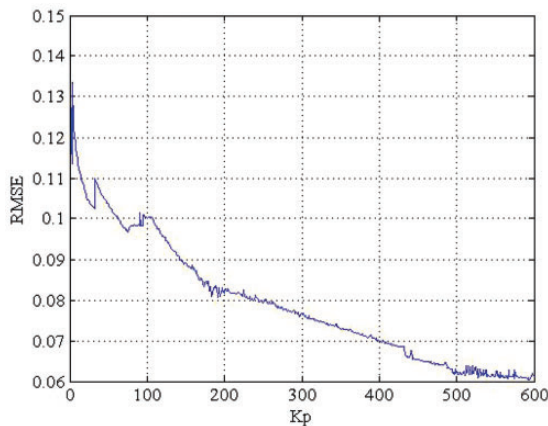


**Figure 13.** RMSE along proportional gain with optimized derivative gain.

when the proportional gain is too high, and adding an optimized derivative gain would no longer improve the system efficiently.

The changes in overshoot after the application of an optimized derivative gain exhibits an interesting trend. The overshoot remains almost constant (around 1% in this case study) as the proportional gain grows. This indicates that adding a derivative controller can provide a consistent overshoot in the system. However,

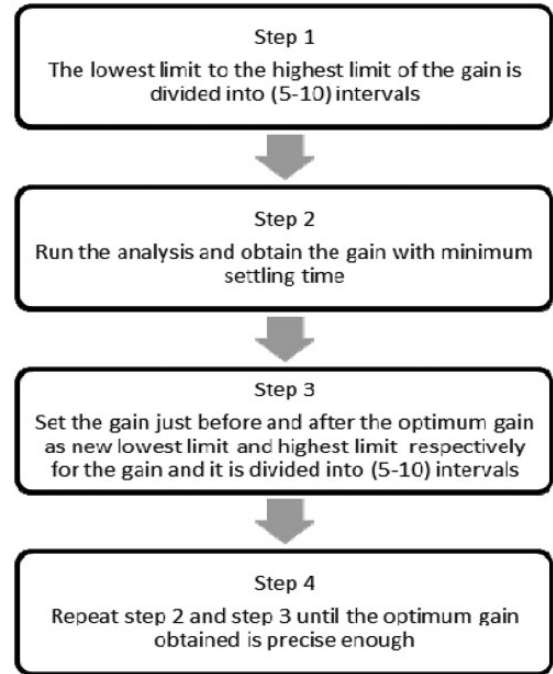


**Figure 14.** Flowchart for tuning proportional gain and derivative gain.

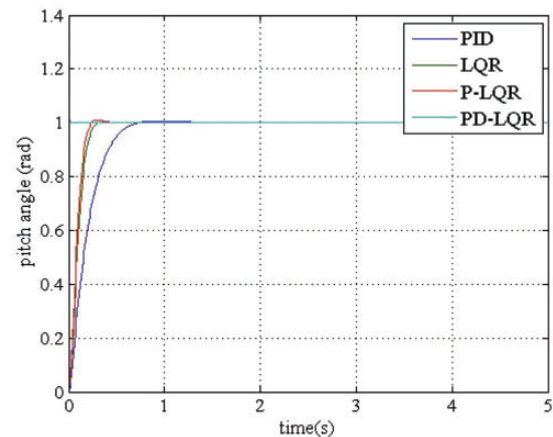


**Figure 15.** Response simulation of the PID, LQR, and PD-LQR controllers.



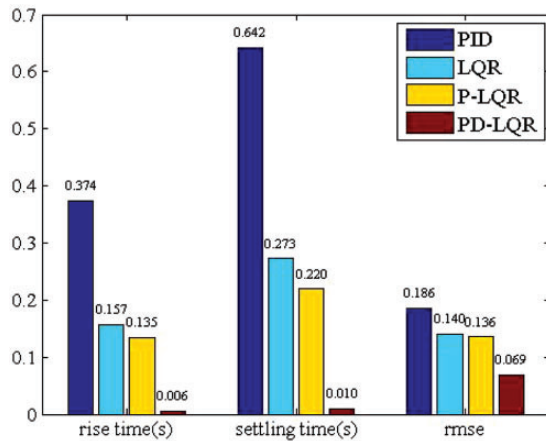


**Figure 16.** Rise time, settling time, and RMSE among controllers.

overshoot would still increase when the proportional gain is over a certain limit (Figure 12).

The steady-state error herein is more stable compared to that shown in Figure 6 because the derivative controller tends to decrease steady-state error as well. Apart from the steady-state error, RMSE also increases when optimized derivative gain is added to the system initially. However, RMSE decreases when proportional gain increases, until the minimal level is reached, as shown in Figure 13. Thus, the selection of an optimum proportional gain with optimized derivative gain for the PD-LQR controller can be concluded with the following characteristics: (1) minimum settling time for the system; and (2) overshoot is still at a consistent value.

### Tuning the proportional and derivative gains of the PD-LQR

Given that derivative gain needs to be optimized for each proportional gain, hundreds or thousands of loops may be involved to obtain the optimized derivative gain for a particular proportional gain. Moreover, the points of proportional gain required for optimization are probably at the thousands. This increases the cost for optimization severely. To reduce this cost, the iteration loop can be designed in a more efficient way as that shown in Figure 14.

The advantage of this method is its use of the least number of loops for performing analysis on the possible values of the gain, from lowest to highest. The gain with the smallest settling time will be chosen; the gains just before and just after the chosen gain will be set as the new lowest limit and the new highest limit of the gain, respectively. The optimum gain will converge to a more precise value as the step is repeated. This method can be used in the optimization of proportional and derivative gains. The proportional and derivative gains in this case study are 426.09 and 1.513, respectively.

**Table 1.** Overshoot and steady-state error among controllers.

Control algorithms	PID	LQR	P-LQR	PD-LQR
Overshoot (%)	0.649	0.351	0.996	0.997
Steady-state error	$8.261 \times 10^{-8}$	$4.509 \times 10^{-5}$	$3.948 \times 10^{-5}$	$9.139 \times 10^{-6}$

PID: proportional-integral-derivative; LQR: linear quadratic regulator; P-LQR: proportional linear quadratic regulator; PD-LQR: proportional-derivative linear quadratic regulator.

**Table 2.** Differences in performance parameter improvements among controllers.

Differences	PID vs. PD-LQR		LQR vs. PD-LQR		P-LQR vs. PD-LQR	
	Value	%	Value	%	Value	%
Rise time (s)	0.368	98.4	0.151	96.2	0.129	95.6
Settling time (s)	0.633	98.5	0.263	96.5	0.210	95.5
RMSE	0.118	63.2	0.072	51.1	0.067	49.3
Steady-state error	~0	~0	~0	~0	~0	~0

PID: proportional-integral-derivative; LQR: linear quadratic regulator; P-LQR: proportional linear quadratic regulator; PD-LQR: proportional-derivative linear quadratic regulator; RMSE: root mean square error.

## Results and discussions

Figure 15 indicates the response simulation of PID, LQR, P-LQR, and PD-LQR. All these controllers try to achieve the desired output. Among all controllers, the PID controller is the slowest to reach the desired output, whereas the PD-LQR controller is the fastest. Figure 16 shows the rise time, settling time, and RMSE of the four controllers. The rise time of the PID controller is 0.374 s while that of the LQR controller is 0.157 s. Although the rise time of the P-LQR controller is 0.135 s, which is lower than that of the PID and LQR controllers, the rise time of the PD-LQR controller is only 0.006 s, or 4.4% of the rise time of the P-LQR controller.

The settling time of the PID controller is 0.642 s, which is the highest among all controllers. The settling time of the LQR controller is 0.273 s, higher than that of the P-LQR controller, which is at 0.220 s. The settling time of the PD-LQR controller is 0.010 s, which is only 4.5% of the settling time of the P-LQR controller. The RMSE of the PID controller remains the highest among the controllers, followed by the LQR, P-LQR, and PD-LQR controllers, respectively. The steady-state errors for all four controllers were close to zero and the difference among them is in the micro range, which is negligible (Table 1). The overshoot of the PID controller is 0.649% while that of the LQR controller is

0.351%. The PD-LQR and P-LQR controllers have almost the same value of overshoot, which were close to 1%. Overshoot is the only aspect wherein the PD-LQR controller has a higher value than both the PID and LQR controllers; however, overshoot of the PD-LQR is still lower than that of the P-LQR controller (Table 1). Nevertheless, the overshoot of PD-LQR controller is within 1.0%, which is within the acceptable range for a UAV. Table 2 shows the improvement of the PD-LQR controller as compared to the PID, LQR, and P-LQR controllers.

## Conclusion

Longitudinal motion control of an UAV is investigated in this paper. PID, LQR, P-LQR, and PD-LQR controllers of the UAV model are studied through simulation which was programmed using Simulink. The comparison of controllers considered the aspects of rise time, settling time, overshoot, steady-state error, and RMSE. The results show that the PD-LQR controller performs better than other controllers in almost all parameters. In future studies, this controller could be applied in a non-linear UAV model to determine its capability for robustness.

## Declaration of conflicting interests

The author(s) declared no potential conflicts of interest with respect to the research, authorship, and/or publication of this article.

## Funding

The author(s) disclosed receipt of the following financial support for the research, authorship, and/or publication of this article: This publication was supported by Universiti Sains Malaysia (Grant No. 304/PAERO/60312047).

## References

- Gao P. On modelling, simulating and verifying a decentralized mission control algorithm for a fleet of collaborative UAVs. *Proc Computat Sci* 2012; 9: 10.
- Han J, Long D, Calvin C, et al. Pitch loop control of a VTOL UAV using fractional order controller. *J Intell Robot Syst* 2014; 73: 9.
- Godbolt BV, Nikolaos I and Alan FL. Experimental Validation of a Helicopter Autopilot Design using Model-Based PID Control. *J Intell Robot Syst* 2013; 70: 15.
- Capello E, Fulvia Q and Roberto T. Randomized approaches for control of QuaRotor UAVs. *J Intell Robot Syst* 2014; 73: 17.
- Wei Y. An operation-time simulation framework for UAV swarm configuration and mission planning. *Proc Computat Sci* 2013; 18: 10.
- Lei G. Safety requirements analysis for control law development of UAV Flight control systems. In: *The 2nd international symposium on aircraft airworthiness (ISAA 2011)*, 2011, vol 17, p.10.
- Khoygani MRR. Designing and simulation for vertical moving control of UAV system using PID, LQR and Fuzzy Logic. *Int J Electric Comput Eng* 2013; 3: 9.
- Honeywell International Inc. *Advanced engine performance and power generation capability for the predator B*, [http://www51.honeywell.com/aero/common/documents/myaerospacecatalog-documents/BA\\_brochures-documents/TPE331-10\\_PredatorB\\_0292-000.pdf](http://www51.honeywell.com/aero/common/documents/myaerospacecatalog-documents/BA_brochures-documents/TPE331-10_PredatorB_0292-000.pdf) (Jun 2009).
- Hajiyev C. LQR controller with Kalman estimator applied to UAV longitudinal dynamics. *Acad J* 2013; 4: 6.
- Joseph MF. *LQG/LTR optimal attitude control of small flexible spacecraft using free-free boundary condition*. Boulder, CO, United States: Aerospace Engineering Sciences Department, University of Colorado, 2006.
- Ahmed WM. Robust hybrid control for ballistic missile longitudinal autopilot. *Chin J Aeronaut* 2011; 24: 12.
- Sartori D, Fulvia Q, Matthew RJ, et al. Implementation and testing of a backstepping controller autopilot for fixed-wing UAVs. *J Intell Robot Syst* 2014; 76: 21.
- Salem M. Robust PID controller design for a modern type aircraft including handling quality evaluation. *Am J Aerospace Eng* 2014; 1: 7.
- Kok KY and Rajendran P. Enhanced longitudinal motion control of UAV simulation by using P-LQR method. *Int J Micro Air Vehicle* 2015; 7: 203–210.
- Lwin N. Implementation of flight control system based on Kalman and PID Controller for UAV. *Int J Sci Technol Res* 2014; 3: 309–312.
- Gong H. Design of automatic climbing controller for large civil aircraft. *J Franklin Instit* 2013; 350: 13.
- Austin R. *Unmanned aircraft systems: UAVS design, development and deployment*. Hoboken, NJ: Wiley Series, 2011, pp.68–69.
- Laila Beebi M, Vishakh KH and Naveen N. Control of longitudinal dynamics in the reentry phase of a reusable launch vehicle. *Int J Adv Res Electr Electron Instrument Eng* 2012; 1: 5.
- Khoygani MRR. Design controller for a class of non-linear pendulum dynamical system. *Int J Artificial Intell* 2013; 2: 10.
- Espinoza T, Alejandro D and Miguel L. Linear and non-linear controllers applied to fixed-wing UAV. *Int J Adv Robot Syst* 2013; 10: 33.
- Czyba R and Grzegorz S. Control structure impact on the flying performance of the multi-rotor VTOL platform – design, analysis and experimental validation. *Int J Adv Robot Sys* 2013; 1: 10.
- Kumar V. Robust LQR controller design for stabilizing and trajectory tracking of inverted pendulum. *Procedia Eng* 2013; 64: 10.
- Kim GB, Trung Kien N, Agus B, et al. Design and development of a class of rotorcraft-based UAV. *Int J Adv Robot Sys* 2013; 10: 1–9.
- Das S. LQR based improved discrete PID controller design via optimum selection of weighting matrices using fractional order integral performance index. *Appl Math Modell* 2013; 37: 16.

25. Torabi A. Intelligent pitch controller identification and design. *J Math Comput Sci* 2014; 8: 15.
26. Nelson RC. *Flight stability and automatic control*, 2nd ed. Boston, MA: McGraw-Hill Education, ISBN 0070462739, 1998.
27. Mishra A. *A study on PID controller design for systems with time delay*. Odisha, India: Department of Electrical Engineering, National Institute of Technology, Rourkela, 2011.

## Nomenclature

$v$	velocity of the UAV (m/s)	$\theta$	pitch angle of the UAV (rad)
$a$	angle of attack of the UAV (rad)	$\delta$	elevator deflection angle (rad)
$q$	pitch rate of the UAV (rad/s)	$K_p$	proportional gain
		$K_i$	integral gain
		$K_d$	derivative gain
		$e(t)$	error at time $t$ (rad)
		$A$	system transition matrix
		$B$	control distribution matrix
		$C$	output matrix
		$D$	feedthrough matrix
		$J$	quadratic performance index
		$K$	optimal feedback gain
		$Q$	positive semi definite matrix
		$R$	positive definite matrix